

# A cost model for green fog computing and networking

Ramon Aparicio-Pardo<sup>1</sup>, Lucile Sassatelli<sup>1</sup>,

<sup>1</sup>Université Côte d'Azur, CNRS, I3S - Sophia Antipolis, France

E-mail: {raparicio,sassatelli}@i3s.unice.fr

## ABSTRACT

5G services and 4K will stress even more the future access/aggregation networks, where video contents have already become the main traffic contributor. The deployment in the convergent access of local micro data-centers (DCs) nodes is one promising approach to successfully manage this challenge. These nodes will be responsible for switching enormous amounts of traffic and simultaneously performing heavy CPU tasks (such as video or radio base band processing). Only a flexible management of these nodes based on NFV, SDN and data analytics will enable to meet these tasks. In this paper, we present a consistent and complete cost model collecting main tradeoffs between energy savings and CPU processing suitable to be used in such a flexible management framework.

**Keywords:** FMC, C-RAN, power model, QoE model, video streaming, cloud/fog computing

## 1. INTRODUCTION

The video streaming share in the Internet traffic is growing at a blistering pace, representing 82% of all traffic by 2020 [1]. Moreover, a part of this growth is associated to the development of high bandwidth demanding applications, e.g. 360° videos (28Mbps [2]).

For access networks (cellular and fixed), this traffic surge is accompanied by a power consumption growth, motivating the need for improving the energy-efficiency of aggregation and access networks. One promising solution is the Fixed-Mobile Convergence (FMC) paradigm [3] (Fig.1 left). The idea behind FMC is to manage jointly the heterogeneous access technologies (e.g., optical, WiFi, 4G) in a unified fixed-mobile convergent optical network to consolidate within the cloud/fog fixed and mobile optical head-ends as well as the base station (base band) processing. The consolidation of the controllers and radio elements is known as Base Band Unit (BBU) hosting, an enabling key element of the FMC: the Cloud Radio Access Network (C-RAN) architecture [3].

The mutualized usage of physical resources (processing, networking equipment and power-consuming cooling infrastructure) allows significantly reducing power consumption. However, that requires fine control of network management to avoid performance losses. The key-enablers for this are Network Function Virtualization (NFV), Software Defined Networking (SDN), that allow fully exploiting the flexibility and scalability of cloud resources.

The management of these networks will have to account for video streaming as the new pivot of user traffic. Most Internet video streaming corresponds to so-called HTTP Adaptive bit rate Streaming (HAS), as the MPEG-DASH standard, that lets the video bit rate to be adapted over time to, e.g., best fit the available client bandwidth.

Augmented ISP nodes with IP routing, optical switching, computation and storage abilities will therefore be the elementary bricks of future ISP telco networks. Based on a thorough literature study, we propose a complete cost model, necessary for any operational design, collecting in a comprehensive way: power, bandwidth, computational costs and video quality.

## 2. NODE ARCHITECTURE

The micro-DC node architecture, depicted in Fig. 1 right, is the conventional 2-(or 3)-tier for DC [4]-[5] (a 2-tier here), with additional optical and electronic networking equipment. We emphasize that the network nodes in Fig.1 left. are these micro-DCs within the ISP network implemented with the hardware in Table 1. The elementary blocks of the node are:

- 1) **DC servers**, which are responsible for carrying out: (i) the video transcoding operations and (ii) the radio baseband operations performed in the Base Band Unit (BBU) at the Base Stations (BSs) in a today's RAN.
- 2) **Electronic networking equipment**, which are the *Ethernet gigaswitches*, interconnecting the servers (first aggregation level of the 2-tier data center); and, the *IP edge routers*, interconnecting the Ethernet gigaswitches (second aggregation level) and providing access to the Internet.
- 3) **Optical networking equipment**, which are the *Optical Cross Connects (OXC)* and the *OEO transponders* responsible for adding, dropping and switching the optical signals. We assume their power contribution as negligible [6].

Table 1. Hardware characteristics of the data center node.

Hardware	Model	Cores $T$	CPU $C^{CPU}$	RAM $C^{RAM}$	Switch. Capacity $C^{ESW}$	Idle Power $P^{STAT}$	Dyn. Power $P^{DYN}$	Servers $K$
Taurus DC server [7]	Intel Xeon e5-2630	2×6 /12	2.3 GHz	32 GB	–	95 W	125 W	16
Ethernet giga-switch [5]	Cisco Catalyst 6509	–	–	–	320 Gbps	1616W	404 W	–
IP edge router [5]	Cisco 7609	–	–	–	560 Gbps	3640 W	910 W	–

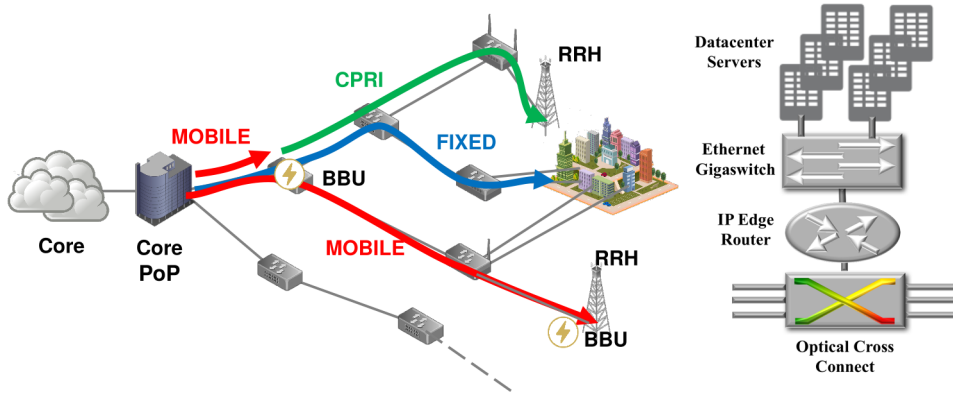


Figure 1. Left: the FMC concept. Right: Network node architecture.

### 3. POWER CONSUMPTION MODEL

The power consumption model of all the elements follows an affine function with two terms: a baseline power (idle power) and variable term depending on load. The baseline power usually accounts cooling, power supply and lightning systems.

#### 3.1 Server Consumption Model

As in [7] the server power consumption is estimated as the sum of a baseline constant term (TDP) plus the dynamic consumption proportional to the number of active cores at the server. A whole core is activated when hosting a Virtual CPU (vCPU). We assume that (i) video transcoding and (ii) radio base band operations are performed by a Virtual Machine (VM) set  $VM$ , where each  $vm \in VM$  requests  $d_{vm}$  vCPUs. The proportionality coefficient with respect to number of active cores is simply the quotient between the maximal dynamic power and the number of cores  $K$ . Then, the total server consumption (static and dynamic)  $P^{CPU}$  is:

$$P^{CPU} = P^{STAT} \cdot PUE + \frac{P^{DYN}}{K} \cdot \sum_{vm \in VM} d_{vm} = 106.4 + 10.417 \cdot \sum_{vm \in VM} d_{vm} \text{ Watts} \quad (1)$$

where PUE is the Power Utilization Efficiency of the cooling equipment at the server chassis (1.12<sup>1</sup>). Finally, we do not consider the storing consumption (e.g. for video caching) as typical values (a few Watts [8]) are negligible with respect to those shown in Table 1.

#### 3.2 Electronic networking equipment

This networking equipment performs their switching operations in the electrical domain, constituting important sources of power consumption. We use the power model described in [5] with the values in Table 1. This model computes the overall consumption  $P^{ESW}$  of these devices following an affine function of the traffic load as:

$$P^{ESW} = P^{STAT} + \frac{P^{DYN}}{C^{ESW}} \cdot f \quad (2)$$

where  $f$  is the amount of Gbps traversing the device,  $P^{STAT}$  is the idle power,  $P^{DYN}$  is the difference between the maximal power consumption and the idle power (i.e. the extra power consumed if the device is fully load) and  $C^{ESW}$  is the maximal equipment capacity in Gbps.

However, values in Table 1 show that the idle power represents ca. 80% the total consumption, justifying to neglect the load dependency and overestimating the total power as the sum of idle and dynamic contributions, i.e. the maximal power consumption when the device is operating at  $C^{ESW}$  Gbps. Using the values in Table 1, the Ethernet gigaswitch power  $P^{EGS}$  and the IP edge router  $P^{IPR}$  power can be computed as:

$$P^{EGS} = P^{STAT} + P^{DYN} = 1614 + 404 = 2020 \text{ Watts} \quad (3)$$

$$P^{IPR} = P^{STAT} + P^{DYN} = 3640 + 910 = 4550 \text{ Watts} \quad (4)$$

#### 3.3 Optical switching equipment

The optical switching equipment consists of OXCs and OEO transponders. The formers are responsible for switching a wavelength channel from an incoming to an outgoing fiber without traversing the electrical domain, i.e. without requiring CPU processing, yielding to much less consumption than their electrical counterpart. We use the model in [6], assuming 80 WDM channels per fiber, where power  $P^{OXC}$  linearly depends on the fiber ports as:

$$P^{OXC} = 150 + 100 \cdot a + 85 \cdot d \text{ Watts} \quad (5)$$

<sup>1</sup><https://www.google.com/about/datacenters/efficiency/internal/>

where  $a$  is the number of add/drop ports and  $d$  is the number of network-side ports. Considering (i) the access/aggregation network as a multi-stage tree topology ( $d=3$ ,  $a=2$ ) and (ii) optical signal are only added/dropped at the end-nodes or at the intermediate nodes performing processing, power  $P^{OXC}$  can be computed as

$$P^{OXC} = \begin{cases} 405 \text{ Watts,} & \text{if node transparently bypasses optical signals} \\ 605 \text{ Watts,} & \text{if node performs electrical (BBU or video) processing} \end{cases} \quad (6)$$

Assuming a OEO transponder ([6]) as a (non-coherent) 10Gbps Transponder/Muxponder, it consumes 40W [9]. Finally, it is worth noticing that these powers are negligible in comparison with the electrical switches powers.

#### 4. BANDWIDTH MODEL FOR RADIO LAST HOP

Since BBU processing tasks are deported to a DC node in the aggregation network as depicted in Fig. 1, traffic coming from the mobile edges is transported over the optical fiber plant using a digital Radio Over Fiber (RoF) interface (typically, CPRI [14]). This section presents the model assumptions about the wireless last hop.

We consider that each mobile edge node in Fig 1 is a BS collecting the traffic of a single macro cell site and providing LTE radio coverage of 3 sectors with 20 MHz bandwidth and  $2 \times 2$  MIMO configuration. Table 2 shows the detailed cell site configuration. For this configuration and for the typical LTE values [11], the bit rate per RB can be computed as in [12] obtaining a value of 759.36 *kbps*. Since our cell site uses 6 antennas (3 sectors with  $2 \times 2$  MIMO) and 100 RBs (20 MHz bandwidth) [13], the maximal aggregated rate at a mobile edge is  $C^{LTE} = 455.62 \text{ Mbps}$  ( $6 \times 100 \times 75.936 \text{ Mbps}$ ).

The LTE traffic is transported between the mobile end node and the deported BBU by CPRI. That implies to transform the radio band signals from analog to digital, entailing CPRI bit rate  $C^{CPRI}$  higher than  $C^{LTE}$ . Assuming CPRI standard sampling frequency of 30.72 *MHz* [13], and sample bit width of 15 [14], the CPRI bit rate (I/Q sample data rate) per antenna is 0.9216 *Gbps* ( $2 \times 15 \times 30.72 \text{ MHz}$ ). Then for our cell site (6 antennas), the maximal aggregated CPRI rate is 5.53 *Gbps* ( $6 \times 0.9216 \text{ Gbps}$ ) carried in the CPRI option 7 ( $C^{CPRI} = 9.83 \text{ Gbps}$ ) [14].

Table 2. Cell site scenario.

# Sectors	LTE Bandwidth	MIMO configuration	Freq. domain usage	CQI Index	Modulation	Code Rate	Spectral efficiency	Quantization	$C^{LTE}$	$C^{CPRI}$
3	20 MHz	$2 \times 2$ MIMO	Full load	13	64 QAM	0.75	4.5234 bps/Hz	24 bit	455.62 Mbps	9.83 Gbps

#### 5. CPU PROCESSING MODEL

The physical servers at the micro-DC nodes of the convergent access perform either Digital Base band preprocessing or Video Transcoding tasks. This section introduces the model used to estimate the CPU needs.

##### 5.1 Digital baseband processing

Baseband processing is carried out at the micro DCs by the VMs (also called Virtual Digital Units, VDU) for the BBU units deported from the cell BSs. We use the model in [10] to find the number of GOPS per BS, which is divided into subcomponents of the digital base band processing equipment whose number of GOPS depends on: bandwidth, spectral efficiency, number of antennas, system load (frequency-domain), number of spatial streams and quantization. Then, the overall number of GOPS is simply computed as the sum for all the digital subcomponent GOPS. For our cell site scenario (Table 2), the overall number of GOPS is 229.2813. From the distributed computing projects *Asteroids@home*<sup>2</sup> and *SETI@home*<sup>3</sup>, we find the GOPS per core used by our servers (Table 1) when signal processing is performed. This figure is close to 2.5 GOPS per core (or vCPU) in both projects, whereby a value of  $d = 91.713$  vCPUs required by the digital baseband processing of each BS.

##### 5.2 Video Transcoding

Transcoding changes the encoding parameters of a video (usually rate and resolution). In this work, we assume that the VMs performing the transcoding tasks at the micro-DCs generates continuous video rates from one unique high quality video version cached at the DC (in this work 1080p and 4K versions). In contrast to standard adaptive streaming (as *MPEG-DASH*) where versions encoded at certain (discrete) different rates are stored, continuous video rate adaptation enables higher QoE at the client at less storing overheads [15], [16].

From [17], the transcoding effort is rather independent from the input and output coding rates and more sensitive to the resolutions. We consider 3 video types with increasing complexity (cartoon, movie and sport). Table 3 shows the number of pass-marks required to transcode a representation of one of the contents in Table 4 from 1080p to 1080, 720 or 360p and from 4K to 4K. These pass-marks values were computed from GHz values in [17], assuming the number of pass-marks for a 1080p transcoding as 2000<sup>4</sup>. The 4K resolution was not covered in [17], but from *community.netgear* forum<sup>5</sup>, it is roughly estimated as four times the CPU effort for 1080p.

<sup>2</sup> [https://asteroidsathome.net/boinc/cpu\\_list.php](https://asteroidsathome.net/boinc/cpu_list.php)

<sup>3</sup> [https://setiathome.berkeley.edu/cpu\\_list.php](https://setiathome.berkeley.edu/cpu_list.php)

<sup>4</sup> <https://support.plex.tv/hc/en-us/articles/201774043-What-kind-of-CPU-do-I-need-for-my-Server-computer->

<sup>5</sup> <https://community.netgear.com/t5/New-to-ReadyNAS/4k-transcoding/td-p/1097311>

The required transcoding vCPUs can be found by dividing the values in Table 3 with the number of pass-marks per core used by our equipment (Table 1). According to *cpubenchmark* website<sup>6</sup>, this figure is 8915/12 (742.9).

Table 3. Transcoding CPU (pass-marks).

	Cartoon	Movie	Sport
<b>360p</b>	620.44	985.40	912.41
<b>720p</b>	1007.30	1299.27	1635.04
<b>1080p</b>	1138.69	1613.14	2000
<b>4K</b>	4554.74	6452.55	8000

Table 4. Videos and corresponding type and resolutions.

Content Type	Video Name [19]	Video Name [20]
	360p, 720p, and 1080p	4K
<b>Cartoon</b>	Big Buck Bunny, Sintel Trailer	Bosphorus
<b>Movie</b>	Old Town Cross	Jockey
<b>Sport</b>	Touchdown Pass, Rush Field Cuts	ReadySetGo

## 6. QUALITY OF EXPERIENCE MODEL

We characterize the users' Quality of Experience (QoE) model as a function depending on the coding parameters (rate and resolution) and on the video content, by means of the Video Quality Metric (VQM) [18], which is a full-reference metric better correlated to human perception than other similar metrics. We use some of the rate-distortion curves (VQM vs coding rate) presented in [[19], Fig. 2] and [[20], Fig. 21]. The exact video sequences are shown in Table 4. Since smaller VQM scores correspond to better QoE values, we normalize these curves between 0 and 1, and we take as QoE function  $1 - \text{VQM score}$  (0 represents the worst QoE; 1, the best). Then, we derive the QoE function by the same power law fitting as in [19], yielding a different concave function of the coding rate, for each resolution and video sequence. If a linear optimization model is targeted, a linear approximation of the QoE function may be considered as:  $QoE = ab + \beta$ ,  $b \in [b_{min}, b_{max}]$ . Table 5 gives the parameters  $\alpha$ ,  $\beta$ ,  $b_{min}$  and  $b_{max}$  for each video and resolution. Recall that  $b$  is the nominal value in *Mbps* of the coding rate.

Table 5. Linearization parameters:  $\alpha$ ,  $\beta$ ,  $b_{min}$ ,  $b_{max}$

	Cartoon				Movie				Sport			
	$\alpha$	$\beta$	$b_{min}$	$b_{max}$	$\alpha$	$\beta$	$b_{min}$	$b_{max}$	$\alpha$	$\beta$	$b_{min}$	$b_{max}$
<b>360p</b>	0.1516	0.6303	0.2	0.7	0.3978	0.6796	0.2	1.7	0.4005	0.6801	0.2	2.2
<b>720p</b>	0.4668	0.6934	0.2	1.7	0.3421	0.8395	0.7	3.2	0.1216	0.6851	0.7	7.2
<b>1080p</b>	0.3456	0.6691	0.2	2.77	0.1336	0.7603	1.2	6.2	0.1238	0.7486	1.2	8.2
<b>4K</b>	0.0499	0.1098	2.2	22.7	0.0466	0.1025	2.2	24.2	0.0443	0.0975	2.2	24.7

## 7. CONCLUSIONS

The exhaustive micro DC model presented in this paper is suitable to be used in future works investigating the beneficial tradeoff of co-locating video and BBU processing in 5G Cloud-RAN, as suggested in [21].

## REFERENCES

- [1] Cisco, "VNI Global IP Traffic Forecast, 2015 - 2020," 2016.
- [2] *Within* application. Available: <http://with.in/>
- [3] European "COMBO" Project. [Online]. Available: <http://www.ict-combo.eu/>
- [4] A. Greenberg, et al., "The cost of a cloud: research problems in data center networks," *ACM SIGCOMM computer communication review*, vol. 39, no. 1, pp. 68–73, 2008.
- [5] A. Vishwanath, et al., "Energy consumption of interactive cloud-based document processing applications," in Proc. *IEEE ICC*, 2013.
- [6] W. VanHeddeghem et al., "Power consumption modeling in optical multilayer networks," *Photonic Netw. Comm.*, vol. 24, no. 2, pp. 86–102, 2012.
- [7] M. Kurpicz, et al., "How much does a VM cost? Energy-proportional Accounting in VM-based Environments," in Proc. *PDP*, Heraklion, Greece, Feb. 2016, p. 8.
- [8] N. Choi et al., "In-network caching effect on optimal energy consumption in content-centric networking," in *IEEE ICC*, Jun. 2012.
- [9] W. Vereecken and B. Lannoo, "Final report: Collection of data about energy consumption in network elements and subsystems," *TREND Deliverable FP7-ICT-257740/D1. 3*, 2012.
- [10] B. Debaillie, et al., "A flexible and future-proof power model for cellular base stations," in *IEEE VTC Spring*, May 2015.
- [11] S. S. Brian Classon, Ajit Nimbalkar and I. Toufik, *LTE - The UMTS Long Term Evolution: From Theory to Practice*. Wiley, 2011
- [12] D. Fooladivanda and C. Rosenberg, "Joint resource allocation and user association for heterogeneous wireless cellular networks," *IEEE Trans. on Wireless Com.*, vol. 12, no. 1, pp. 248–257, 2013.
- [13] T. Innovations, "LTE in a nutshell," *White paper*, 2010.
- [14] C. Specification, "V7. 0, Common Public Radio Interface (CPRI), interface specification, 2015," *CPRI Specification*, vol. 7.
- [15] S.-H. Shen and A. Akella, "An information-aware QoE-Centric mobile video cache," in *ACM Mobicom*, 2013.
- [16] E. Baik, et al., "VSync: Cloud based video streaming service for mobile devices," in *IEEE Infocom*, 2016.
- [17] R. Aparicio-Pardo et al., "Transcoding live adaptive video streams at a massive scale in the cloud," in *ACM MMSys*, 2015.
- [18] VQM software. [Online]: <https://www.its.bldrdoc.gov/resources/video-quality-research/request-software.aspx>
- [19] L. Toni, et al., "Optimal set of video representations in adaptive streaming," in *ACM MMSys*, 2014.
- [20] M. Uhrina, et al., "Impact of h. 264/AVC and h. 265/HEVC compression standards on the video quality for 4K resolution," *Adv in Electrical and Electronic Eng.*, vol. 12, no. 4, p. 368, 2014.
- [21] M. Sheng, et al., "Video delivery in heterogeneous CRANs: architectures and strategies," *IEEE Wireless Comm. Mag.*, vol. 22, no. 3, pp. 14–21, June 2015.

<sup>6</sup> <http://www.cpubenchmark.net>